A Mathematical Study of Physarum polycephalum

Group members: Charlie Brummitt, Isabelle Laureyns, Tao Lin, David Martin*, Dan Parry, Dennis Timmers, Alexander Volfson, Tianzhi Yang, Haley Yaple

Mentor: Lou Rossi

Abstract

The adaptive and problem solving abilities of Physarum polycephalum have been modeled by Tero, et al using a graph theoretic model and Poiselle flow.[4] We test this model analytically and numerically, and we propose and test an optimality condition to be satisfied by this model. Finally, we analyze the bifurcation associated with the nonlinear term μ in the Tero model.

1 The Tero Model

The amoeboid slime mold Physarum polycephalum is known to exibit remarkable problem solving abilities, including solving mazes and Steiner trees in an a manner that significantly reduces unnecessary energy expenditure.[3] Early on, this adaptive behavior was described in terms of intelligence and information processing.[1] Most notably, Toshiyuki Nakagaki, et al have earned recognition for experimentally inducing this organism to solve a maze on its own. Initially, the organism was grown on the entire maze. As food in the maze grew scarce, food sources were placed at both exits to the maze. When this occurred, the organism contracted inside the maze, removing all links that were unnecessary to connect the two food sources, and retaining a single link through the maze that connected the two food sources. Moreover, the link maintained was consistently found to be the shortest of two possible routes.[2] In addition to finding minimum length routes, it was soon shown that the Physarum plasmodium works to maximize fault tolerance. This behavior is an example of ad-hoc networking, which is in many respects more robust and flexible than top-down networking.

A mathematical model for this phenomenon based on a relationship between the flux of chemical gradients and the diameter of transport tubes has recently been introduced by Tero, et al[4], and is currently under study for potential

*Contact at dwmath@gmail.com.

applications to infrastructure, including highways, railways, communications networks, and even biological computing.[6][5]

Tero represented the organism as a graph in which vertices represent the food sources and the nodes, while edges represent the connecting channels in the organism (See Figure 1). Vertex i is associated with a net flux m_i and a net pressure p_i - the former being a fixed parameter of the system, and the latter being dependent on the nature of the channels leading out of the node. The edge connecting vertex i to vertex j has length L_{ij} and radius a_{ij}.

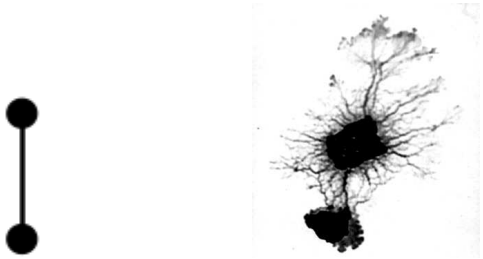

Figure 1: The vertices represent food sources around which the organism is bundled, Edges represent tubing connecting these sections. Additional vertices, which we refer to as "nodes" may represent branches in the tubing.

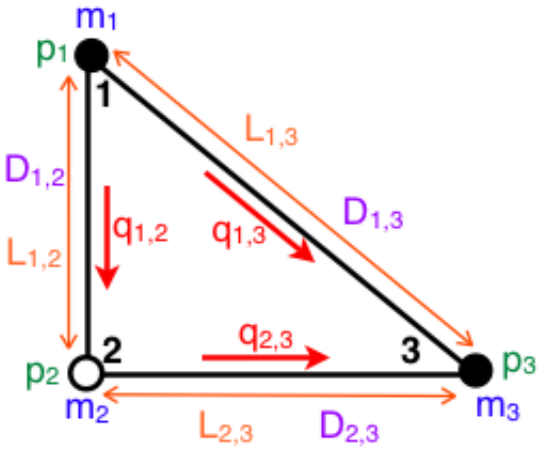

Figure 2: Example of a three vertex network. The filled in dots represent a source and a sink, while the empty dot represents a node. Tube lengths are labeled in orange; tube sizes in purple; tube fluxes in red; source fluxes in blue; and associated pressures in green.

The flow is characterized by a very low Reynalds number, and as such, flow through the channel is approximated as Poiselle flow. Thus, the flux through edge ij is given by

$$q_{ij} = \frac{a_{ij}^4}{8\pi L_{ij}\kappa}(p_i - p_j) \tag{1}$$

where κ is the viscosity of the fluid. For simplicity,

$$D_{ij} = \frac{a_{ij}^4}{8\pi\kappa}$$

was chosen instead of a_{ij} as the parameter charactizing the thickness of the channel. Then

$$q_{ij} = \frac{D_{ij}}{L_{ij}}(p_i - p_j) \tag{2}$$

This relation is subject to the constraint that flow is conserved.

$$\sum_{j \in N_i} q_{ij} = m_i \tag{3}$$

and

$$\sum_{N_i} m_i = 1 \tag{4}$$

Tero postulated that the diameter of the tubes satisfies a differential relation similar to that for swarm intelligence.[4] Namely, tubes undergo a natural exponential decay, which is counterbalanced by a growth that is dependent on the flux through the tubes, as seen in equation 5.

$$\frac{dD_{ij}}{dt} = rD_{\max}f(|q_{ij}|) - rD_{ij} \tag{5}$$

Tero then proposed two possible choices for the growth function, f, given in equations 6 and 7.

$$f(x) = ax^{\mu} \tag{6}$$

$$f(x) = \frac{ax^{\mu}}{1 + ax^{\mu}} \tag{7}$$

Equation 6 is simple and therefore conducive to precise analysis, while Eq. 7 is more realistic because it is limited to $f(x) < 1$ regardless of μ. As such, the former will be studied in our analytic approach, while the latter will be studied in our computational analysis.

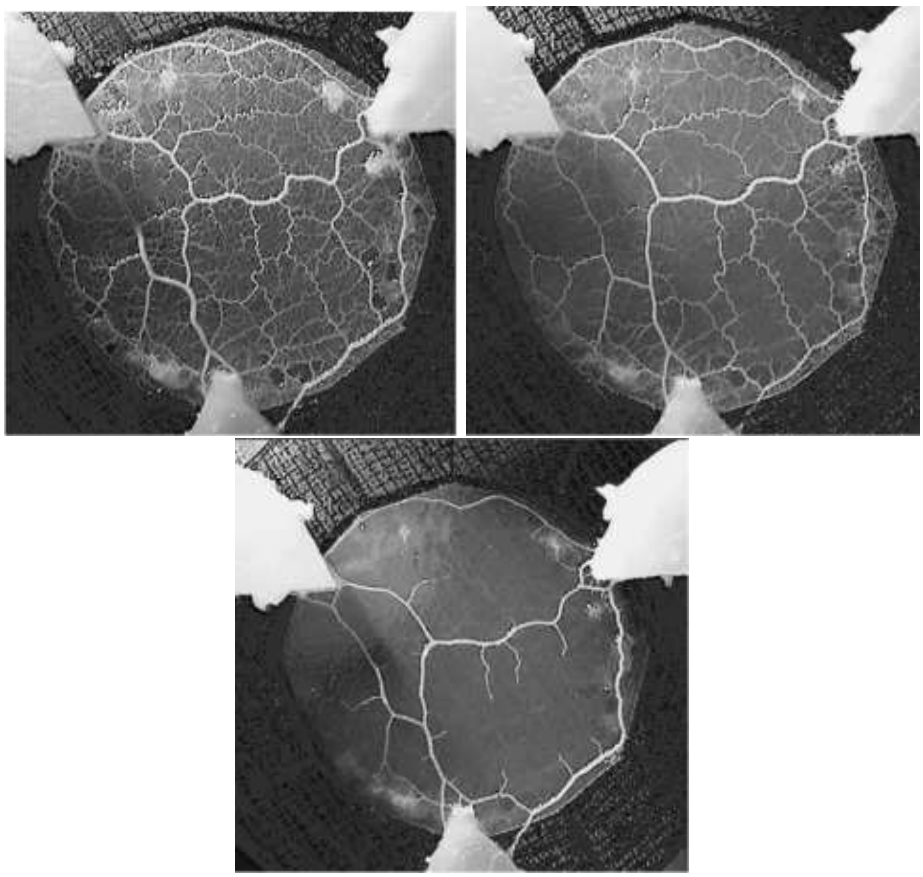

Figure 3: Physarum polycephalum in a petri dish with three food sources placed around the edge. Initially, the organism fills the dish with an extensive network. As time progresses, however, most of the edges networks decay, except for a few that are most useful.

2 Analytic Results

2.1 Method

Given an initial state of the diameters D_{ij} of the tubes, the system is going to evolve according to 5. In this section we analytically compute the steady states of the diameters. For large graphs, this problem is too difficult to solve analytically. As such, we address the simple case of a two node graph - one source and one sink. Node 1 is a source with net flux 1 and associated pressure P. Node 2 is a sink with net flux -1, and with a pressure which we set to zero. In that case, we have fluxes, q_i through the respective edges, which have lengths

L_i. Then Eq. 2 gives

$$q_i = \frac{D_i}{L_i} P$$

By using Eq. 3, we can solve explicitly for P, in terms of tube sizes and tube lengths. This, in turn enables us to obtain the fluxes explicitly as functions of the D_i's and the L_i's. By putting these into Eq. 5, we obtain explicit formulas for the derivatives

$$\frac{dD_i}{dt} = F(D_i)$$

where we use $f(x) = bx^{\mu}$. By setting these formulas to 0, we can obtain the fixed points. The stability of the fixed points may then be analyzed by computing the eigenvalues of the Jacobian

$$J = \left(\frac{dF(D_i)}{dD_j} \right)$$

If these eigenvalues are all negative, then the fixed point is stable, and hence represents a steady-state of the graph. Otherwise, the fixed point does not represent a steady-state.

The results will strongly depend on whether $\mu < 1$ or $\mu > 1$. Two different cases are considered, when the nodes are connected by two or three edges (see Figure 4).

2.2 Two edge model

The first case we consider is when the edge lengths are the same, i.e. $L_1 = L_2 = L$. We find by Eq. 5 that

$$m = q_1 + q_2 = L^{-1}(D_1 + D_2)P,$$

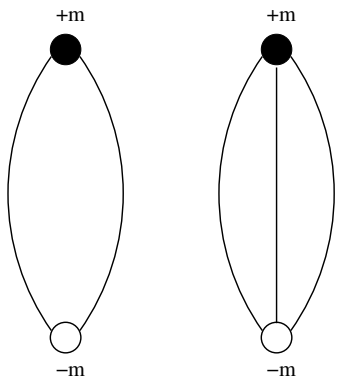

Figure 4: The two-node network

Therefore, the pressure P is given by

$$P = \frac{mL}{D_1 + D_2}. \tag{8}$$

In order for the RHS of 5 to be zero for both D_1 and D_2 it follows that

$$\frac{D_i}{D_{\max}} = a\Big(\frac{D_i}{L}P\Big)^{\mu}, \qquad \text{for } i = 1, 2. \tag{9}$$

There are three solutions to this equation. First, if $D_1 = 0$ then $q_1 = 0$ and $q_2 = m$ so that

$$D_2 = aD_{\max}|q|^{\mu} = aD_{\max}m^{\mu}.$$

Similarly, there is a fixed point $D_1 = aD_{\max}m^{\mu}$ and $D_2 = 0$. Finally, if $D_2 \neq 0$ then by dividing (9) for $i = 1$ and $i = 2$ we obtain

$$\frac{D_1}{D_2} = \Big(\frac{D_1}{D_2}\Big)^{\mu},$$

And since $\mu \neq 1$ the diameters are equal $D_1 = D_2$. Furthermore, since the lengths of the edges are the same, so are the fluxes: $q_1 = q_2 = m/2$. The diameters of the tubes are

$$D_1 = D_2 = aD_{\max}(m/2)^{\mu}.$$

Having found the fixed point, the next step is to compute the Jacobian. The Jacobian has the form

$$J^1 = \begin{pmatrix} D_1^{\mu-1}C_{11} & C_{12} \\ C_{21} & D_2^{\mu-1}C_{22} \end{pmatrix}.$$

The Jacobian was computed using Mathematica, the code and all the entries of J^1 can be found in Appendix A. Here we would just like to consider the behavior of J^1 on the diagonals.

Start with the case $\mu < 1$. The powers of D_i on the diagonal of J^1 are $\mu - 1 < 0$. The Jacobian is singular at either $D_1 = 0$ or $D_2 = 0$. We study the Jacobian for $D_1 = \epsilon$ and consider the dynamics as $\epsilon \to 0$. The three remaining terms are $O(1)$.

$$J^1 = \begin{pmatrix} \epsilon^{-1} & O(1) \\ O(1) & O(1) \end{pmatrix}.$$

For ϵ small, the above matrix has an eigenvalue of $+1$. Since the system has a positive eigenvalue, the fixed point with $D_1 = 0$ is unstable. Similarly, the fixed point with $D_2 = 0$ is unstable.

It remains to study the case when $D_1 = D_2 = aD_{\max}(m/2)^\mu$. Again using Mathematica we obtain that at this point the Jacobian has an eigenvalue -1 with multiplicity 2. Hence, leaving both edges in the graph results in a stable fixed point.

The remaining case is when $\mu > 1$. In this case we do not find any singularities and we can evaluate the Jacobian at the fixed points. The results are summarized in Table 1. In either case that $D_1 = 0$ or $D_2 = 0$, the eigenvalue -1 has multiplicity 2. Hence, closing either one of the edges results in stable fixed points. Leaving both edges open results in an unstable fixed point.

	remove one edge	keep all edges
$\mu < 1$	$-1, +1$ (unstable)	$-1, -1$ (**stable**)
$\mu > 1$	$-1, -1$ (**stable**)	$-1, u-1$ (unstable)

Table 1: Stability: eigenvalues for two equal length edges

As a consequence, both edges will remain in use for $\mu < 1$, while $\mu > 1$ implies that only one edge will be used.

2.3 Three edge model

Suppose the edge lengths are the same, i.e. $L_1 = L_2 = L_3 = L$. We find by 5 that

$$m = q_1 + q_2 + q_3 = L^{-1}(D_1 + D_2 + D_3)P$$

and thus

$$P = \frac{mL}{D_1 + D_2 + D_3}. \tag{10}$$

In order for the RHS of 5 to be zero for both D_1, D_2 and D_3 we find

$$\frac{D_i}{D_{\max}} = a\Big(\frac{D_i}{L}P\Big)^\mu, \qquad \text{for } i = 1, 2, 3. \tag{11}$$

There are seven solutions to this equation which correspond keeping all edges, closing one edge or closing two edges. By symmetry it suffices to consider three distinct cases. Namely closing the first two tubes, closing the first tube or keeping all tubes open.

If $D_1 = D_2 = 0$, then $q_1 = q_2 = 0$ or $q_3 = m$ so that

$$D_3 = aD_{\max}|q_3|^\mu = aD_{\max}m^\mu.$$

In case $D_1 = 0$, then by dividing (11) for $i = 2$ and $i = 3$ we obtain

$$\frac{D_2}{D_3} = \Big(\frac{D_2}{D_3}\Big)^{\mu},$$

And since $\mu \neq 1$ we find $D_2 = D_3$. Furthermore, since the lengths of the edges are the same we find $q_2 = q_3 = m/2$. Hence, we find

$$D_1 = D_2 = aD_{\max}(m/2)^{\mu}.$$

The last case is when neither of the tubes is closed. By dividing (11) for $i = 1$, $i = 2$ and $i = 2$, $i = 3$ we find

$$\frac{D_1}{D_2} = \Big(\frac{D_1}{D_2}\Big)^{\mu}, \qquad \frac{D_2}{D_3} = \Big(\frac{D_2}{D_3}\Big)^{\mu},$$

and again $D_1 = D_2 = D_3$ so that $q_1 = q_2 = q_3 = m/3$ and

$$D_1 = D_2 = D_3 = aD_{\max}(m/3)^{\mu}$$

Having found these fixed points we then have to evaluate the Jacobian at these fixed points. We find that the Jacobian has the form

$$J^2 = \begin{pmatrix} D_1^{\mu-1}C_{11} & C_{12} & C_{13} \\ C_{21} & D_2^{\mu-1}C_{22} & C_{23} \\ C_{31} & C_{32} & D_3^{\mu-1}C_{33} \end{pmatrix}.$$

The Jacobian was computed using Mathematica, the code and all the entries of J^2 can be found in Appendix A. Here we would just like to consider the behavior of J^2 on the diagonals.

First we study the case when $\mu < 1$. As before, the Jacobian is singular when at least one of the $D_i's$ is set to zero. Consider the dynamics by setting $D_1 = \epsilon$ and letting $\epsilon \to 0$. We find that the Jacobian has an eigenvalue of $+1$ and thus has at least one positive eigenvalue. Setting both D_1 and D_2 equal to ϵ and letting $\epsilon \to 0$ we find that the Jacobian has an eigenvalue of $+1$ with multiplicity 2. We check the eigenvalues when setting $D_1 = D_2 = D_3 = aD_{\max}(m/3)^{\mu}$ and find that the Jacobian has eigenvalue -1 with multiplicity 3. Hence, this is the only stable fixed point.

It remains to study the case when $D_1 = D_2 = D_3 = aD_{\max}(m/3)^{\mu}$. Again using Mathematica we obtain that at this point the Jacobian an eigenvalue -1 with multiplicity 2. Hence, leaving both edges in the graph results in a stable fixed point.

	remove two edges	remove one edge	keep all edges
$\mu < 1$	$-1, +1, +1$ (unstable)	$-1, +1, ?$ (unstable)	$-1, -1, -1$ (**stable**)
$\mu > 1$	$-1, -1, -1$ (**stable**)	$-1, -1, u-1$ (unstable)	$-1, u-1, u-1$ (unstable)

Table 2: Stability: eigenvalues for three edges equal in length

The remaining case is when $\mu > 1$. In this case we do not find any singularities and we can evaluate the Jacobian at the three fixed points. We find that if $D_1 = D_2 = D_3 \neq 0$, then the eigenvalues are equal to -1 and $\mu - 1$, the later with multiplicity 2, so the point is unstable. In the case $D_1 = 0$ and $D_2 = D_3 \neq 0$, the eigenvalues are $+1$ and $\mu - 1$ the former with multiplicity 2. Therefore, the latter two fixed points are unstable. Finally, if $D_1 = D_2 = 0$ then -1 is the only eigenvalue with multiplicity 3 which is thus stable. Hence, closing any two out of three edges is the only way to obtain stable fixed points. We have summarized the results in Table 2.

As before, we find that for $\mu < 1$, the only stable state uses all paths, while for $\mu > 1$, the only stable state uses exactly one path. This is in agreement with Tero's results [4], and supports the idea that Physarum polucephalum is accurately modeled by functions using $\mu > 1$.

3 Numerical Results

For our numerical computations, we uses a semi-implicit scheme

$$A(D_{i,j}^n)P^{n+1} = B$$
$$D_{i,j}^{n+1} = \frac{1}{1+dt}(D_{i,j}^n + dt\, f(Q_{i,j}^n(D_{i,j}^n, P^{n+1}))$$

Implemented in Matlab.

3.1 4 Node Asymmetric Model

We begin by analyzing a 4 node asymmetric model with a single source and a single sink, separated by 2 nodes, as shown in Figure 5. We introduce a slight asymmetry, making one of the edges a little longer.

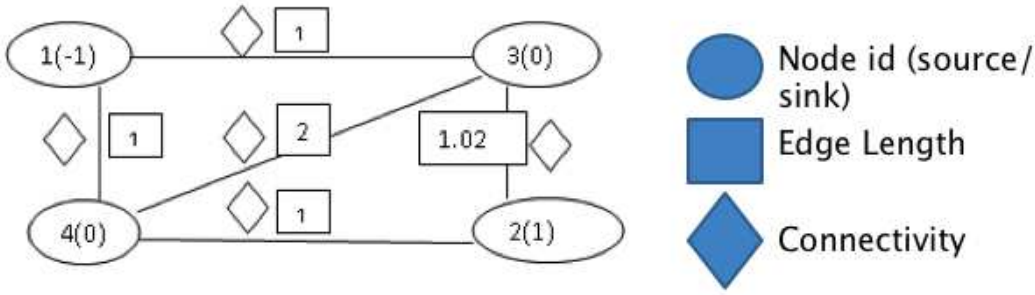

Figure 5: Four Node Asymmetric Circuit.

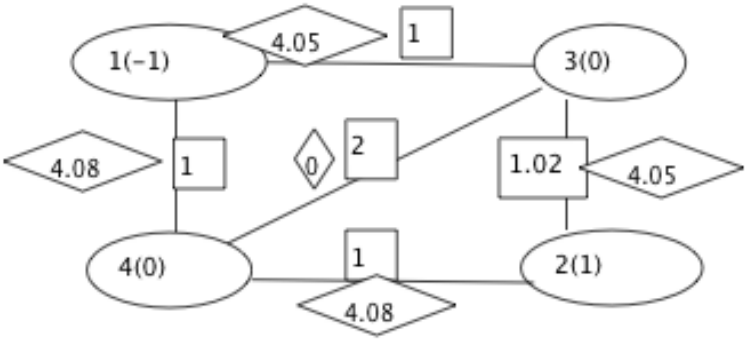

Figure 6: $\mu = 0.8$

We run the code first for $\mu = 0.8 < 1$ (Figure 6), and discover that all edges are used - although the shorter edges are used more heavily than the longer ones. On the other hand, with $\mu = 1.8 > 1$ (Figure 7), only the shortest route is taken.

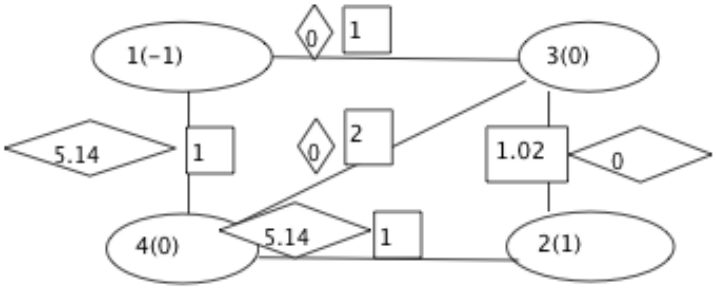

Figure 7: $\mu = 1.8$

3.2 4 Node Symmetric Model

Next, we take the same graph, but make it completely symmetric. Here, the

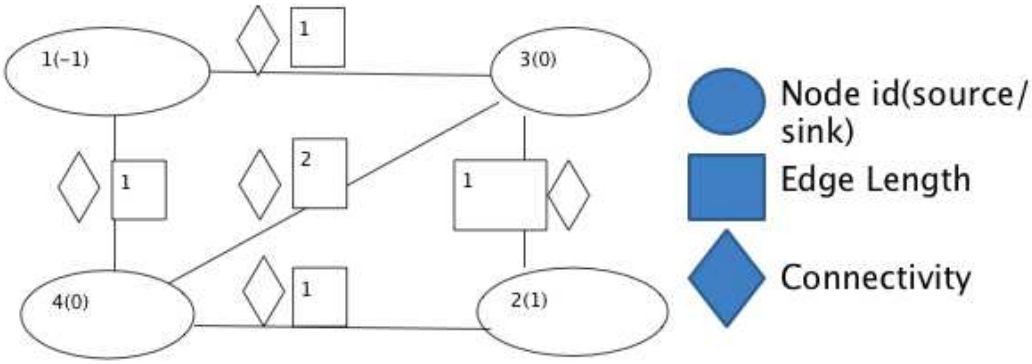

Figure 8: Four Node Symmetric Circuit.

case $\mu = 0.8 < 1$ results in flow using both routes to the sink in a manner that is completely symmetric (Figure 9). On the other hand, when μ is set to $\mu = 1.8 > 1$, one of the paths again vanishes (Figure 10). It is unclear how one path is chosen over the other, but we strongly suspect that it is due to small-scale asymmetries at or near computer precision.

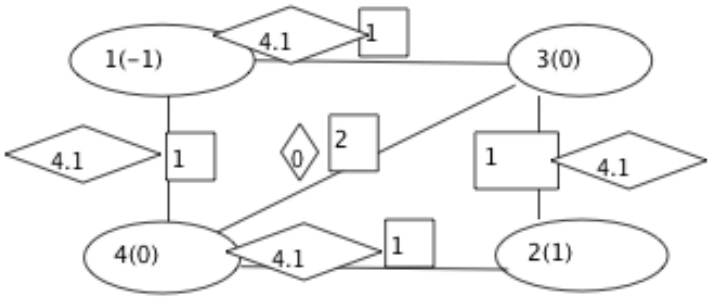

Figure 9: $\mu = 0.8$

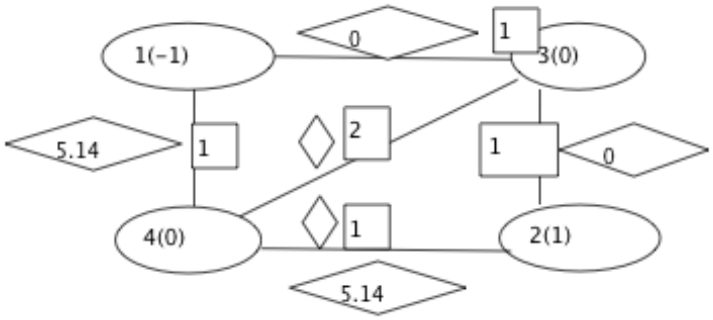

Figure 10: $\mu = 1.8$

3.3 Periodic Source/Sink

Next, we replace the constant values of ± 1 with a periodic source and sink, of $\pm \cos t$ (Figure 11). This is designed to better reflect the biological reality of fluxuating flow, as described by Tero [4]. The result for $\mu = 0.8 < 1$ is that after a short transitional phase, all paths are equally used (Figure 12). For $\mu = 1.5 > 1$, however, we again find that after a short transitional phase, all routes die down except for one (Figure 13). Finally, we analyze the bifurcation associated with μ, by plotting the connectivity of the various paths against μ (Figure 14). For $\mu < \mu_0 \approx 1.52$, both paths are used about equally. But when $\mu > \mu_0$, one route falls off sharply, while the other route assumes all of the flow. This is at odds with Tero's observations, which place the bifurcations closer to $\mu_0 = 1.15$. However, it may also be expected that the bifurcation properties of μ vary from graph to graph.

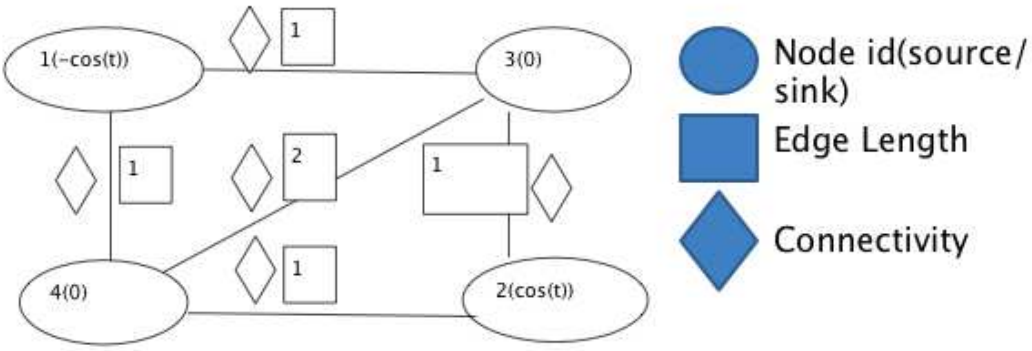

Figure 11: Periodic Source/Sink.

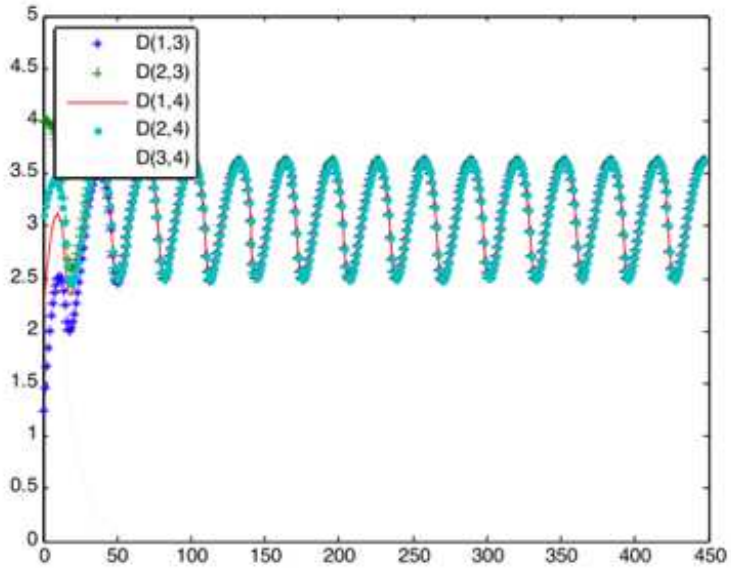

Figure 12: $\mu = 0.8$

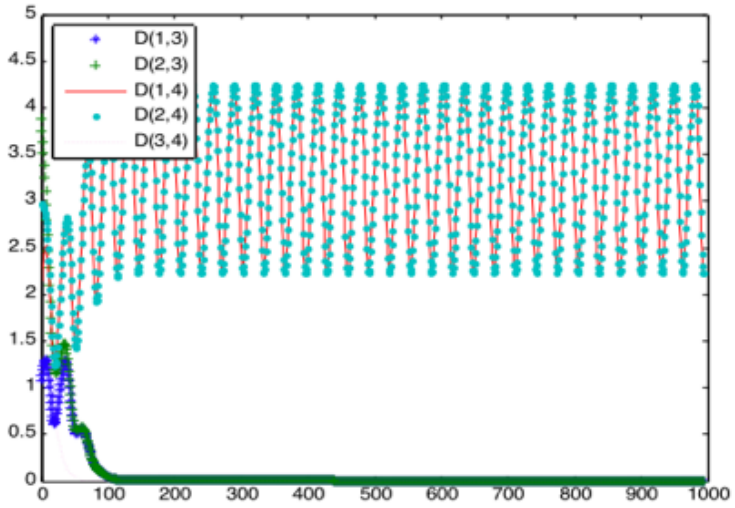

Figure 13: $\mu = 1.5$

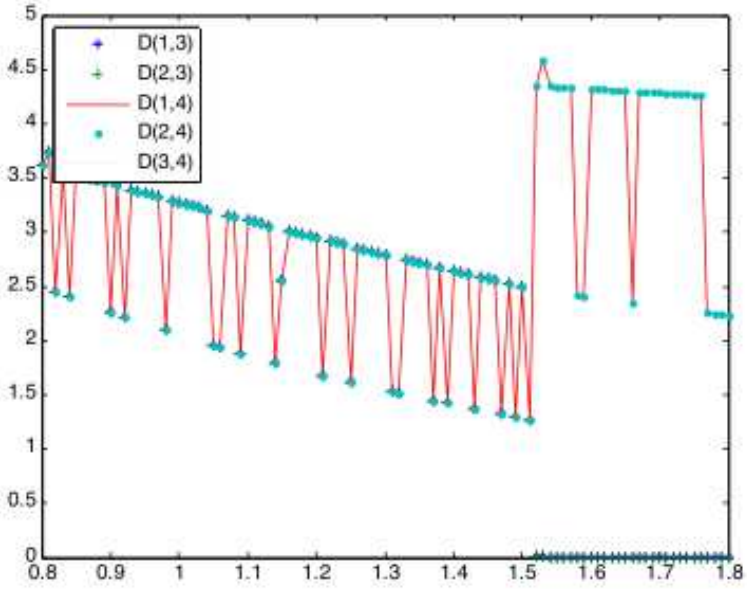

Figure 14: μ versus connectivity

3.4 The Maze Model

We conclude our numerical analysis with a more substantial example - namely, the maze of Nakagaki [2], shown in Figure 15.

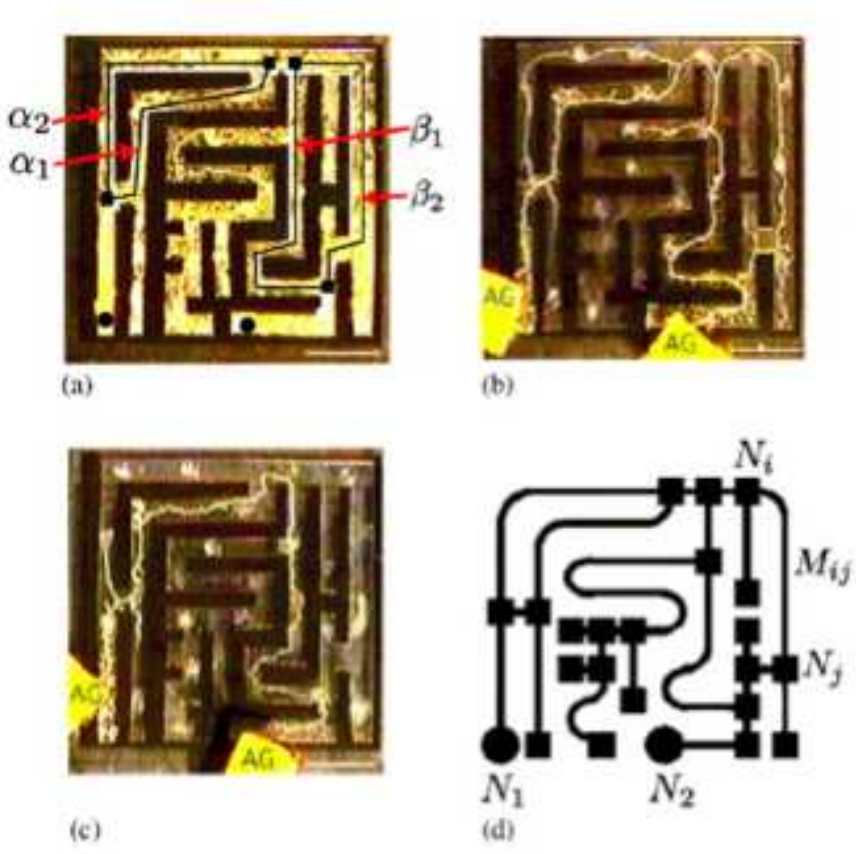

Figure 15: Photographs of Nakagaki's Maze. Physarum polycephalum is initially grown on the entire maze (a). Then food sources are placed at either end of the maze (b). As food within the maze becomes scarce, the organism contracts unnecessary pathways, keeping only the shortest pathway connecting the two food sources (c). In (d), a graph is drawn to model the maze. The circles correspond to food sources(i.e. sources/sinks), while the boxes represent nodes.

For our purposes, we use a slightly simplified graph (Figure 16). In the case of $\mu = 0.8$, we find that unnecessary dead-end nodes are disused and die, but all other paths are used, including longer routes (Figure 17). However, when $\mu = 1.8$, all routes die out except the one representing the shortest distance between the source and sink - except for one case, in which one route is used principally by the organism, while its alternate, of equal length, retains a very small level of connectivity (Figure 18).

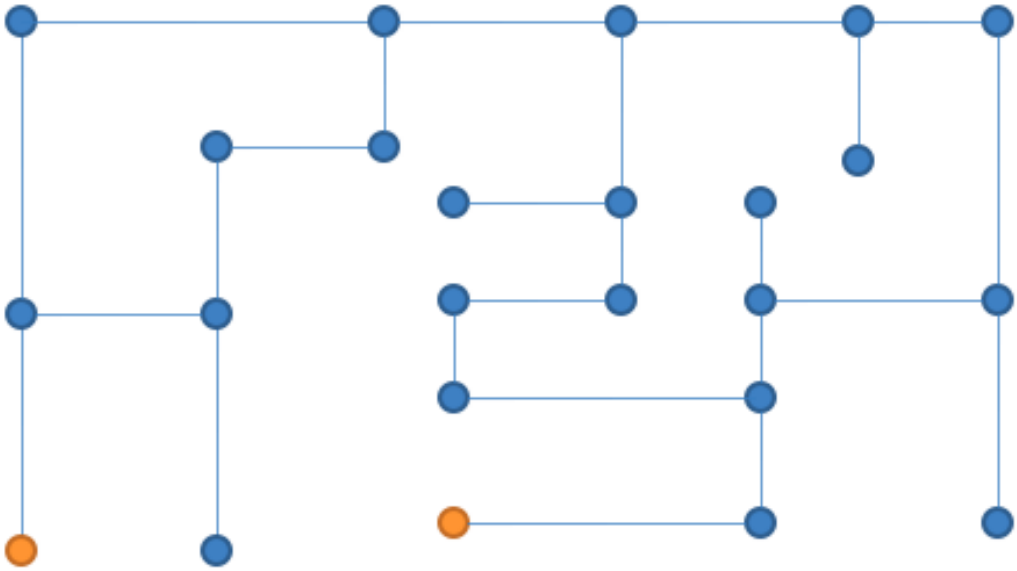

Figure 16: Maze Setup: The yellow vertices are the source/sink, while the blue vertices are the nodes.

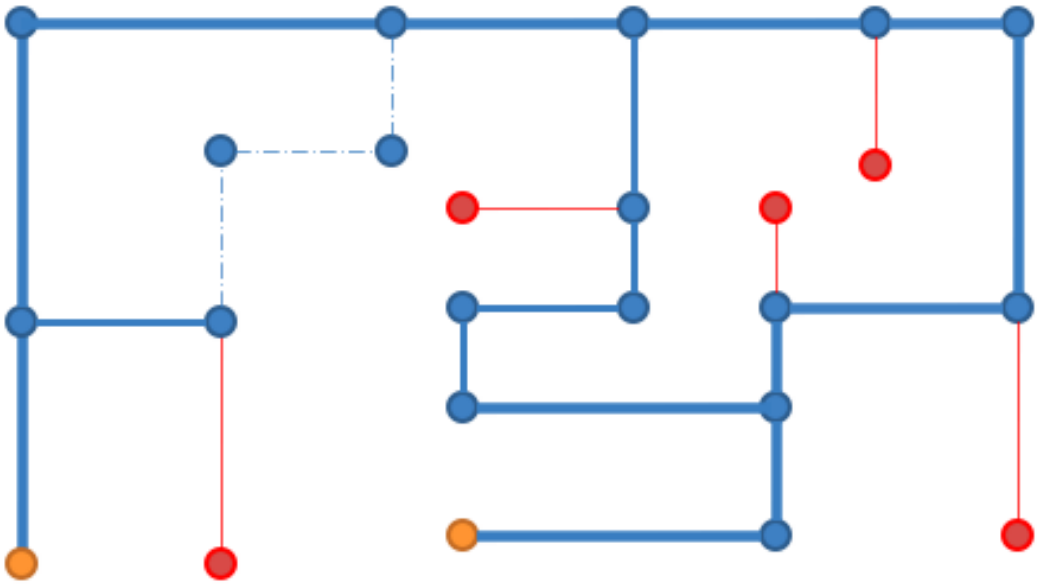

Figure 17: $\mu = 0.8$. Red edges and nodes have lost their connectivity, while blue edges and nodes retain their connectivity.

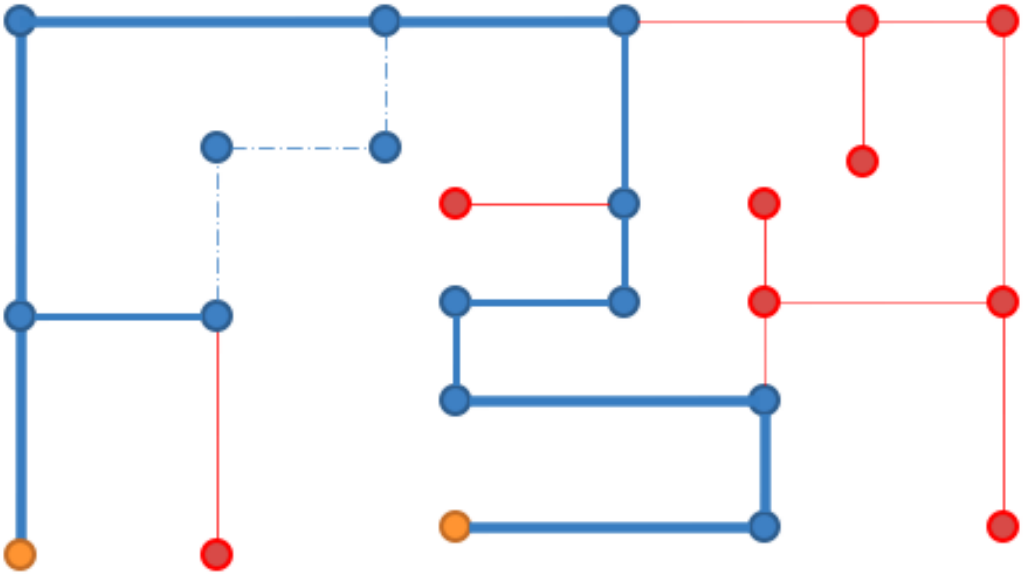

Figure 18: $\mu = 1.8$. Red edges and nodes have lost their connectivity, while blue edges and nodes retain their connectivity. The dotted edges retain very little connectivity.

4 Optimality

Two optimality conditions have been studied in connection with Physarum polycephalum: robustness, i.e. fault tolerance, and the total length of the tubing.[3] We propose another optimality condition which measures total transport against energy expended. The transport is the integral of magnitude of flux throughout the entire network.

$$\text{Total Transport: } \sum_{i,j} |q_{i,j}|\, L_{i,j}$$

Actually, a factor of $\frac{1}{2}$ should be added because edges are counted twice in the expression above. However, this will not affect our analysis and is ignored. Meanwhile, the energy used in maintaining the network will vary with tube size and length.

$$\text{Energy Used: } \sum_{i,j} D_{i,j}\, L_{i,j}$$

If we divide these, we obtain a quantity that we believe the organism would like to maximize.

$$\text{Want to maximize: } \frac{\text{total transport}}{\text{energy used}} = \frac{\sum_{i,j} |q_{i,j}|\, L_{i,j}}{\sum_{i,j} D_{i,j}\, L_{i,j}}$$

Note, however, that this quantity is not unitless. This problem can be corrected by a multiplicative factor. Then we are interested in computing following quantity, which we refer to as the "Energy ratio."

$$\text{Energy Ratio: } \max_{\{D_{i,j} \,:\, D_{i,j} \in \text{steady states}\}} \frac{\sum_{i,j} |q_{i,j}|\, L_{i,j}}{\sum_{i,j} D_{i,j}\, L_{i,j}}$$

5 Bifurcation

To analyze the change in the network near $\mu = 1$, we studied the bifurcation diagram of the 3 node network shown in Figure 19. Using *Mathematica*, we derived the three-dimensional ordinary differential equation for $(D_{12}(t), D_{13}(t), D_{23}(t))$ by symbolically solving for the pressures p_1, p_2, p_3, which is possible for such a simple network because it only requires inverting a 2×2 matrix. Moreover, we use the more realistic growth function below.

$$\text{Growth function: } f(x) = \frac{ax^{\mu}}{1 + ax^{\mu}}$$

Since our numerical simulations suggest that the system always converges to a fixed point, we decided to solve for fixed points (rather than more complicated behavior, such as limit cycles or chaos). Our goal was to study the fixed points as a function of the nonlinearity parameter, μ.

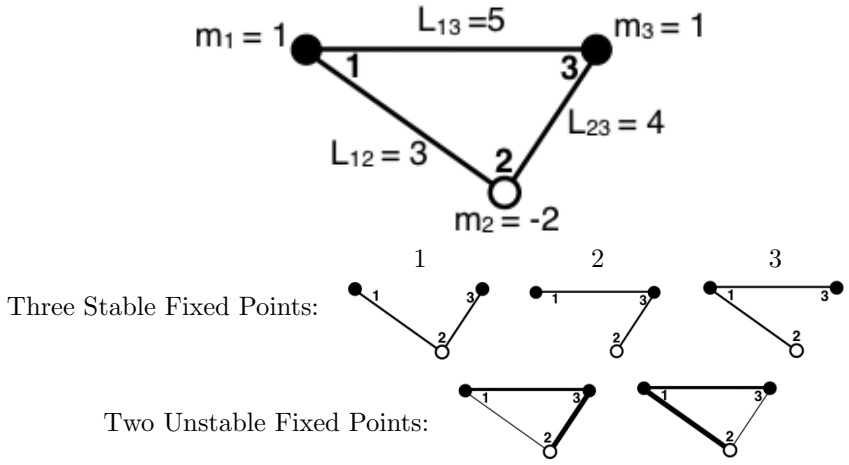

Figure 19: A three node graph for stuying bifurcation.

For integer values of μ, *Mathematica* can (in principle) solve for all of the fixed points, not just one of them, using the function `NSolve`. Thus we solved for the five fixed points of $(D_{12}(t), D_{13}(t), D_{23}(t))$ at $\mu = 2$. To find the fixed points at arbitrary μ, we used the so-called "continuation method" for finding new fixed points: by changing μ in small steps (say, 0.01), numerically find new fixed points using the old fixed points as initial guesses (using, say, Newton's method). This allows us to track how the five fixed points at $\mu = 2$ change as we increase μ to 10 and decrease μ to 0. The bifurcation diagram that results is shown in Fig. 20.

We draw two important conclusions from the bifurcation diagram in Fig. 20. First, the two unstable curves (dashed lines) merge with two stable curves near approximately $\mu \approx 2.5$. Below this bifurcation, the unstable fixed points have a singularity in their derivatives, but we suspect this effect is spurious because the stable fixed points with which they merge do not have a singularity. Second, the two most optimal fixed points are linearly unstable. That is, the most optimal configurations of the network are *not* attained by the Tero model. These two optimal yet unstable fixed points have all three diameters positive (i.e., all tubes open). This suggests that in larger networks, for larger μ using *fewer* paths is more stable. We hypothesize that bifurcation diagrams of larger networks would confirm this: for large μ, even though using many paths may be more optimal, it's not a linearly stable configuration, and so the network uses fewer paths, which is linearly stable.

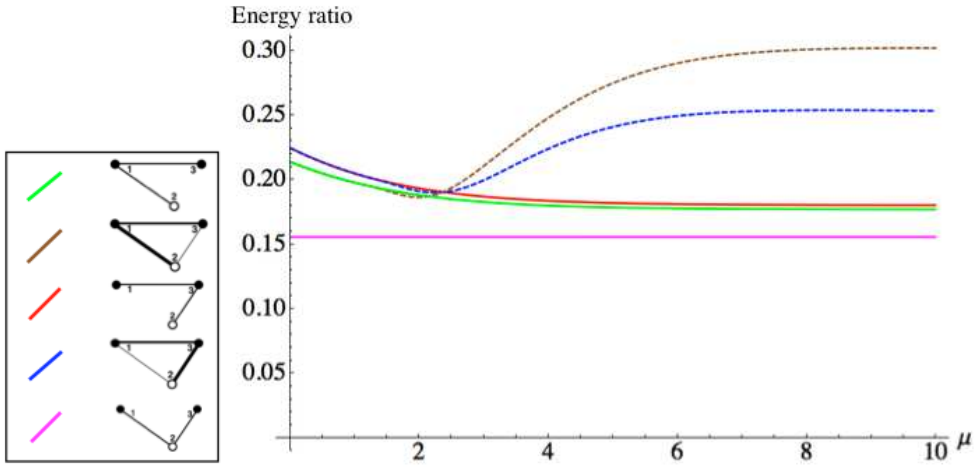

Figure 20: Bifurcation diagram of the five fixed points of the diameters D_{ij} of the L8R network at $\mu = 2$, traced back to $\mu = 0$ and forward to $\mu = 10$ via the iterative "continuation method," which finds roots using the previous root as a guess. The two unstable fixed points are plotted in dashed lines, while the three stable fixed points are plotted in solid lines.

6 Conclusions

Algebraic computations agree with numerical simulations that the Tero model accurately models the behavior of Physarum polycephalum, for $\mu \approx 1.8$. We also were able to confirm Tero's findings that lower values of μ resulted in full networks, while higher values of μ cause the network to thin out. This is even more significant, as specifically we confirmed the observed behavior of Nakagaki's maze, and we tested the behavior of the model for the case of an alternating source/sink, which better mimics Tero's description of the biological reality of flow, which varies in a noise-like fashion.

The exact point of this bifurcation does not, however, appear to be consistent for different graphs. Furthermore, our optimality condition did not produce the results that are intuitively expected. A few possible improvements are as follows.

1. Total transport and Energy expenditure could be analyzed separately, leading to more specific and meaningful insight.

2. Total energy expenditure was related to the quantities $D_{ij}L_{ij}$. This does not appear to lead to a physically meaningful quantity, as D_{ij} has units of Length to the fourth power. Possibly, the energy expenditure in maintaining the network of tubes is more directly related to either the surface area of the tubes $\sim D_{ij}^{1/4}L_{ij}$, or the volume $\sim D_{ij}^{1/2}L_{ij}$.

Finally, we note that the bifurcation behavior of Tero's model with respect to μ is more subtle than initially expected. In our algebraic analysis, we obtained bifurcation exactly at $\mu = 1$. In our numerical simulations, however, we obtained bifurcation at $\mu \approx 1.52$, while in our bifurcation diagram we obtained bifurcation at $\mu \approx 2.5$. Considering the fact that we used different graphs for all three cases, it is quite possible that this reflects inherent differences in the way the model behaves for different graphs. One possible suggestion for future research is to analyze the bifurcation behavior of the same graph using different methods (i.e. analytic, numerical).

A Mathematica code for the two-node model

Two node/ two edge model

We define the pressure and our driving function when the two edges have the same length.

```
Pr22[m_]:=mL/(D1+D2);
q22[i_, m_]:=Di/L Pr22[m];
f22[i_, m_, a_, μ_]:=Dmax a q22[i, m]^μ - Di;
```

```
Pr22[m]
q22[1, m]
f22[2, m, a, u]
```

$$\frac{Lm}{D_1+D_2}$$

$$\frac{mD_1}{D_1+D_2}$$

$$-D_2 + a\left(\frac{mD_2}{D_1+D_2}\right)^u D_{\max}$$

We construct the Jacobian

```
Jac22 = Table[FullSimplify[D[f22[i, m, a, μ], Dj]], {i, 1, 2}, {j, 1, 2}];
MatrixForm[Jac22]
```

$$\begin{pmatrix} -1 + \frac{am\mu D_2\left(\frac{mD_1}{D_1+D_2}\right)^{-1+\mu} D_{\max}}{(D_1+D_2)^2} & -\frac{a\mu\left(\frac{mD_1}{D_1+D_2}\right)^{\mu} D_{\max}}{D_1+D_2} \\ -\frac{a\mu\left(\frac{mD_2}{D_1+D_2}\right)^{\mu} D_{\max}}{D_1+D_2} & -1 + \frac{am\mu D_1\left(\frac{mD_2}{D_1+D_2}\right)^{-1+\mu} D_{\max}}{(D_1+D_2)^2} \end{pmatrix}$$

Note that on the diagionals we get terms ${D_i}^{u-1}$. Hence, as explained in the report, if μ <1, then the Jacobian has a positive eigenvalue when setting either D_1 or D_2 equal to zero. So for μ <1 we only have to test the case when

Simplify [Eigenvalues [Jac22/.$D_1 \to aD_{\max}(m/2)^\mu$/.$D_2 \to aD_{\max}(m/2)^\mu$]]

$\{-1, -1+\mu\}$

Hence, if μ <1 this is the only stable state. However, if μ >1 the above would be unstable but setting either D_1or D_2 equal to zero would be stable.

Eigenvalues [Simplify [Jac22/.$D_1 \to aD_{\max}m^\mu$/.$D_2 \to 0, \mu > 1$]]

$\{-1, -1\}$

Two node/ three edge model

We define the pressure and our driving function when the two edges have the same length.

Pr23[m_]:=$\frac{mL}{D_1+D_2+D_3}$;
q23[i_, m_]:=$\frac{D_i}{L}$Pr23[m];
f23[i_, m_, a_, μ_]:=$D_{\max}$aq23[i, m]$^\mu - D_i$;

Pr23[m]
q23[1, m]
f23[2, m, a, u]

$\frac{Lm}{D_1+D_2+D_3}$

$\frac{mD_1}{D_1+D_2+D_3}$

$-D_2 + a\left(\frac{mD_2}{D_1+D_2+D_3}\right)^u D_{\max}$

We construct the Jacobian

Jac23 = Table [FullSimplify [D [f23[i, m, a, μ], D_j]] , {i, 1, 3}, {j, 1, 3}] ;
MatrixForm[Jac23]

$$\begin{pmatrix} -1 + \frac{am\mu(D_2+D_3)\left(\frac{mD_1}{D_1+D_2+D_3}\right)^{-1+\mu}D_{\max}}{(D_1+D_2+D_3)^2} & -\frac{a\mu\left(\frac{mD_1}{D_1+D_2+D_3}\right)^{1+\mu}D_{\max}}{mD_1} & \cdots \\ -\frac{a\mu\left(\frac{mD_2}{D_1+D_2+D_3}\right)^{1+\mu}D_{\max}}{mD_2} & -1 + \frac{am\mu(D_1+D_3)\left(\frac{mD_2}{D_1+D_2+D_3}\right)^{-1+\mu}D_{\max}}{(D_1+D_2+D_3)^2} & \cdots \\ -\frac{a\mu\left(\frac{mD_3}{D_1+D_2+D_3}\right)^{1+\mu}D_{\max}}{mD_3} & -\frac{a\mu\left(\frac{mD_3}{D_1+D_2+D_3}\right)^{1+\mu}D_{\max}}{mD_3} & \cdots \end{pmatrix}$$

$$\begin{pmatrix} \cdots & -\frac{a\mu\left(\frac{mD_1}{D_1+D_2+D_3}\right)^{1+\mu}D_{\max}}{mD_1} \\ \cdots & -\frac{a\mu\left(\frac{mD_2}{D_1+D_2+D_3}\right)^{1+\mu}D_{\max}}{mD_2} \\ \cdots & -1+\frac{am\mu(D_1+D_2)\left(\frac{mD_3}{D_1+D_2+D_3}\right)^{-1+\mu}D_{\max}}{(D_1+D_2+D_3)^2} \end{pmatrix}$$

Note that on the diagionals we get terms ${D_i}^{u-1}$. Hence, as explained in the report, if μ <1, then the Jacobian has a positive eigenvalue when setting either D_1 or D_2 or D_3 equal to zero. Thus, we only test the case when

Simplify [Eigenvalues [Jac23/.$D_1 \to aD_{\max}(m/3)^{\mu}$/.$D_2 \to aD_{\max}(m/3)^{\mu}$/.$D_3 \to aD_{\max}(m/3)^{\mu}$]]

$\{-1, -1+\mu, -1+\mu\}$

Therefore, when μ <1 this is the only stable state. However, if μ >1 the above would be unstable. Another case would be to set $D_1 = 0$ which turns out to be unstable. However, we need to make small changes to `Jac23` by hand (by multiplying out the powers of D_i in top and bottom).

We can test the other fixed points. The first being closing tube 1 which has has eigenvalue of μ-1 and is therefore unstable.

$$\mathbf{T1} = \begin{pmatrix} -1+\frac{am\mu(D_2+D_3)\left(\frac{mD_1}{D_1+D_2+D_3}\right)^{-1+\mu}D_{\max}}{(D_1+D_2+D_3)^2} & -\frac{a\mu\left(\frac{m}{D_1+D_2+D_3}\right)^{1+\mu}(D_1)^{\mu}D_{\max}}{m} & \cdots \\ -\frac{a\mu\left(\frac{mD_2}{D_1+D_2+D_3}\right)^{1+\mu}D_{\max}}{mD_2} & -1+\frac{am\mu(D_1+D_3)\left(\frac{mD_2}{D_1+D_2+D_3}\right)^{-1+\mu}D_{\max}}{(D_1+D_2+D_3)^2} & \cdots \\ -\frac{a\mu\left(\frac{mD_3}{D_1+D_2+D_3}\right)^{1+\mu}D_{\max}}{mD_3} & -\frac{a\mu\left(\frac{mD_3}{D_1+D_2+D_3}\right)^{1+\mu}D_{\max}}{mD_3} & \cdots \end{pmatrix}$$

$$\begin{pmatrix} \cdots & -\frac{a\mu\left(\frac{m}{D_1+D_2+D_3}\right)^{1+\mu}(D_1)^{\mu}D_{\max}}{m} \\ \cdots & -\frac{a\mu\left(\frac{mD_2}{D_1+D_2+D_3}\right)^{1+\mu}D_{\max}}{mD_2} \\ \cdots & -1+\frac{am\mu(D_1+D_2)\left(\frac{mD_3}{D_1+D_2+D_3}\right)^{-1+\mu}D_{\max}}{(D_1+D_2+D_3)^2} \end{pmatrix};$$

Eigenvalues [FullSimplify [T1/.$D_1 \to 0$/.$D_2 \to aD_{\max}(m/2)^{\mu}$/.$D_3 \to aD_{\max}(m/2)^{\mu}, \mu > 1$]]

$\{-1, -1, -1+\mu\}$

Finally, the last fixed point is made stable by closing of all but one tube.

$$\mathbf{T2} = \begin{pmatrix} -1+\frac{am\mu(D_2+D_3)\left(\frac{mD_1}{D_1+D_2+D_3}\right)^{-1+\mu}D_{\max}}{(D_1+D_2+D_3)^2} & -\frac{a\mu\left(\frac{m}{D_1+D_2+D_3}\right)^{1+\mu}(D_1)^{\mu}D_{\max}}{m} & \cdots \\ -\frac{a\mu\left(\frac{m}{D_1+D_2+D_3}\right)^{1+\mu}(D_2)^{\mu}D_{\max}}{m} & -1+\frac{am\mu(D_1+D_3)\left(\frac{mD_2}{D_1+D_2+D_3}\right)^{-1+\mu}D_{\max}}{(D_1+D_2+D_3)^2} & \cdots \\ -\frac{a\mu\left(\frac{mD_3}{D_1+D_2+D_3}\right)^{1+\mu}D_{\max}}{mD_3} & -\frac{a\mu\left(\frac{mD_3}{D_1+D_2+D_3}\right)^{1+\mu}D_{\max}}{mD_3} & \cdots \end{pmatrix}$$

$$\begin{array}{lll} \cdots & -\frac{a\mu\left(\frac{m}{D_1+D_2+D_3}\right)^{1+\mu}(D_1)^{\mu}D_{\max}}{m} & \\ \cdots & -\frac{a\mu\left(\frac{m}{D_1+D_2+D_3}\right)^{1+\mu}(D_2)^{\mu}D_{\max}}{m} & \\ \cdots & -1+\frac{am\mu(D_1+D_2)\left(\frac{mD_3}{D_1+D_2+D_3}\right)^{-1+\mu}D_{\max}}{(D_1+D_2+D_3)^2} & \end{array}\Bigg);$$

Eigenvalues [Simplify [T2/.$D_1 \to 0$/.$D_2 \to 0$/.$D_3 \to aD_{\max}m^{\mu}, \mu > 1$]]

$\{-1, -1, -1\}$

References

[1] *Environment-Dependent Self-Organization of Positional Information Field in Chemotaxis of Physarum Plasmodium*: Yoshihiro Miyake; Sunao Tabata; Hirofumi Murakami; Masafumi Yano; and Hiroshi Shimizu; Journal of Theoretical Biology 178 (1996) 341 353

[2] *Maze-solving by an amoeboid organism*: Toshiyuki Nakagaki; Hiroyasu Yamada; Agota Toth; Nature (Vol 407) 28 September 2000

[3] *Obtaining multiple separate food sources: behavioural intelligence in the Physarum plasmodium*: Toshiyuki Nakagaki, Ryo Kobayashi, Yasumasa Nishiura and Tetsuo Ueda; The Royal Society; 20 October 2004

[4] *A mathematical model for adaptive transport network in path finding by true slime mold*: Atsushi Teroa; Ryo Kobayashia; Toshiyuki Nakagaki; Journal of Theoretical Biology 244 (2007) 553564.

[5] *Minimal model of a cell connecting amoebic motion and adaptive transport networks*: Yukio-Pegio Gunji; Tomohiro Shirakawa; Takayuki Niizato; Taichi Haruna; Journal of Theoretical Biology 253 (2008) 659 667

[6] *Rules for Biologically Inspired Adaptive Network Design*: Atsushi Tero; Seiji Takagi; Tetsu Saigusa; Kentaro Ito; Dan P. Bebber; Mark D. Fricker; Kenji Yumiki; Ryo Kobayashi; Toshiyuki Nakagaki1; www.sciencemag.org; Feb 6, 2010